International Journal of Science and Research (IJSR)
ISSN: 2319-7064
ResearchGate Impact Factor (2018): 0.28 | SJIF (2019): 7.583

Assessment of the Stability of the North Western Flank of the Ruashi II Open Pit Mine Southeast of the City of Lubumbashi - *Numerical Approach*

Mwamba Masangu Eric[1], Kasongo wa Mutombo Portance[2], Mukoko Kalenda Gustave [1], Kaniki Tshamala Arthur[3]

[1, 3]Materials Mechanics Laboratory, Polytechnic Faculty, University of Lubumbashi, Lubumbashi, DR Congo

[2]Department of Geology, Faculty of Sciences, University of Lubumbashi, Lubumbashi, DR Congo

[4]Environmental Laboratory, Polytechnic Faculty, University of Lubumbashi, Lubumbashi, DR Congo

Abstract: ***The main objective of this study was to analyze the geometric parameters of the northwestern flank of the Ruashi II mine in relation to the geomechanical characteristics of the host rock if they are respected. This flank experienced a slope failure of the stopes slopes that washed away 177m3 of earth, which hampered the mining operations for several months. To do this, modeling based on the measurements of discontinuities, discriminated a family of stratification whose orientation is 87/311, two families of breaks oriented 77/45 and 46/117 and a westward sliding plane whose orientation parameters are 44/300. Samples taken from the three formations on the flank up to the current operating level have been used to determine the geomechanical parameters that were used to assess the margin of safety with respect to the rupture. After implementation of the 2D model obtained on the area under study by performing two cuts, the result showed that the safety factor was satisfactory. The landslide that occurred at the Ruashi II site is due to the saturation of the soil by the infiltration of runoff water through the tensile cracks in the Saprolite. This resulted in a decrease in cohesion and an increase in specific weight in the geological formations. For its protection, a surface drainage upstream of the unstable zone by digging gullies and percolation drains at the foot of the bleachers is to be considered.***

Keywords: Ruashi, Mine, Lubumbashi, Geomechanics

1. Introduction

The knowledge of the physico-mechanical characteristics of the deposits allows, based on in situ tests or on laboratory samples, to determine the angles of the slopes and special oscillation techniques, which allow a very precise control of the edges of the quarries of an open pit mine which is of great importance for the stability of the mining works [**1**]. In an open pit mine, uncontrolled instability and movement of materials are risk factors (safety factors, social factors, environmental factors [**2**] [**3**]. Recently, a rockfall of a flank wall that occurred was at the root of several material damages, as well as the stoppage of mining works at the Ruashi site. As a consequence, the expected decrease in production at the mine has been reduced, while [**4**] shows that rock mechanics is an important discipline for the rational management of resources. Our study addresses the question of whether it was the cause of the landslide in the middle of mining operations. The lack of a monitoring plan and/or a poor dimensioning of the structures would be the cause of this landslide [**5**] [**1**]. To carry out this study, a geostructural survey was carried out along the flank for interpretation [**6**], and laboratory analysis of the samples for the determination of the values of the characteristic properties of the rock [**7**]. The objective is to analyze the geometrical parameters of the flank in accordance with the geo-mechanical characteristics of the host rock followed by a digitization of the zone for the evaluation of the flank safety factor.

2. Site of Investigation, Materials and Methods

The Ruashi mine is located seven kilometers from downtown Lubumbashi. Itis located between longitudes 270 30' and 270 40' East and latitudes 110 30' and 110 40' South. The surface data offrentis a particularly interesting source of information for the construction of a numerical model since it allows direct and relatively precise observation of the underground structures [**8**] [**9**]. This information mainly concerns the nature of the rocks, their composition and the geometry and orientation of the structural units that compose them [**10**]. These structural units were taken with a geotechnical compass along the northwestern flank of the mine on the observed breaks and fractures. Samples submitted for laboratory analysis provided mechanical information according to NF P 94-071-1 [**11**], NF P 94-420 [**12**]. The description of the materials was used to obtain the mechanical parameters of the rocks. Slide will be of importance in the exploitation of these data for the analysis of stability on the basis of geometrical and geomechanical parameters in order to deduce the safety factor. The stereographic projection is a mode of representation and abstract geometrical construction which analyzes the orientation relationships of tectonic elements in space, [**13**] and the exploitation of structural data will be developed by the stereographic projection software Dips [**14**] for the statistical analysis of discontinuities, determination of the sliding direction [**15**]. Flank data for the discontinuities, whose dip and direction of dip have been tabulated, and data from sets of discontinuities are grouped in **Tables 1 and 2**.

Table 1: Measurements of stratification directions and dips

Direction	Pendage	Sens	Dip	Dip Direction	Direction	Pendage	Sens	Dip	Dip Direction
N145E	20	SW	20	235	N132E	70	NE	70	42
N70E	48	SW	48	160	N136E	71	NE	71	46
N127E	50	SW	50	217	N130E	72	NE	72	40
N93E	40	SW	40	183	N134E	45	NE	45	44
N125E	72	SW	72	215	N122E	60	NE	60	32
N123E	44	SW	44	213	N133E	56	NE	56	43
N125E	46	SW	46	215	N138E	45	NE	45	48
N121E	25	SW	25	211	N131E	65	NE	65	41
N125E	90		90	215	N135E	80	NE	80	45
N122E	70	SW	70	212	N135E	65	NE	65	45
N121E	70	SW	70	211	N123E	55	NE	55	33
N110E	70	SW	70	200	N145E	76	NE	76	55
N105E	60	SW	60	195	N131E	85	NE	85	41
N115E	40	SW	40	205	N136E	80	NE	80	46
N121E	82	SW	82	211	N128E	78	NE	78	38
N129E	85	SW	85	219	N143E	85	NE	85	53
N125E	88	SW	88	215	N140E	85	NE	85	50
N134E	87	SW	87	224	N154E	70	NE	70	64
N136E	85	SW	85	226	N130E	66	NE	66	40
N133E	90		90	223	N134E	50	NE	50	44
N135E	86	SW	86	225	N130E	50	NE	50	40
N152E	84	SW	84	242	N132E	45	NE	45	42
N86E	54	SE	54	176	N140E	60	NE	60	50
N20E	36	SE	36	110	N125E	45	NE	45	35
N76E	52	SE	52	166	N126E	54	NE	54	36
N145E	90		90	235	N112E	35	NE	35	22
N66E	49	NW	49	336	N164E	60	NE	60	74
N120E	90		90	210	N121E	88	NE	88	31
N122E	80	SW	80	212	N140E	78	NE	78	50
N130E	80	SW	80	220	N157E	90		90	67
N120E	85	SW	85	210	N149E	85	NE	85	59
N130E	72	SW	72	220	N134E	90		90	44
N124E	72	SW	72	214	N135E	40	NE	40	45
N110E	40	SW	40	200	N141E	70	NE	70	51
N157E	65	SW	65	247	N144E	72	NE	72	54
N120E	69	SW	69	210	N147E	90		90	57
N116E	71	SW	71	206	N148E	82	SW	82	238

Table 2: Measurements of break directions and dips

Direction	Pendage	Sens	Dip	Dip Direction	Direction	Pendage	Sens	Dip	Dip Direction
N67E	44	NW	44	337	N147E	38	SW	38	237
N58E	41	NW	41	328	N103E	10	SW	10	193
N74E	20	NW	20	344	N132E	42	SW	42	222
N140E	12	SW	12	230	N135E	20	SW	20	225
N78E	29	NW	29	348	N130E	11	SW	11	220
N66E	61	NW	61	336	N42E	38	NW	38	312
N59E	25	NW	25	329	N65E	41	NW	41	335
N46E	35	NW	35	316	N4E	60	NW	60	274
N80E	22	NW	22	350	N8E	63	NW	63	278
N165E	19	SW	19	225	N0E	79	W	79	270
N53E	30	SW	30	143	N40E	86	SE	86	130
N2E	50	SW	50	92	N42E	75	SE	75	132
N31E	61	NW	61	301	N59E	79	SE	79	149
N100E	26	SW	26	190	N24E	84	SE	84	114
N12E	32	NW	32	282	N46E	76	SE	76	136
N96E	35	SW	35	186	N41E	76	SE	76	131
N83E	46	SE	46	173	N34E	70	SE	70	124
N75E	46	NW	46	345	N1E	34	SE	34	91
N91E	55	NW	55	361	N6E	30	SE	30	96
N80E	35	NW	35	350	N48E	77	SE	77	138
N58E	59	NW	59	328	N55E	80	SE	80	145
N95E	51	SW	51	185	N38E	83	SE	83	128
N168E	65	SW	65	258	N174E	39	SW	39	264
N2E	60	SE	60	92	N30E	37	NW	37	300

N165E	34	SW	34	255	N53E	82	SE	82	143
N5E	45	NW	45	275	N35E	55	NW	55	305
N63E	75	SE	75	153	N43E	53	NW	53	313
N44E	83	SW	83	134	N61E	69	SE	69	151
N76E	54	SE	54	166	N37E	85	NW	85	307
N15E	64	NW	64	285	N20E	53	NW	53	290
N67E	44	NW	44	157	N35E	50	NW	50	305
N58E	41	NW	41	148	N164E	85	SW	85	254
N74E	20	NW	20	164	N34E	70	NW	70	304
N140E	12	SW	12	230	N35E	73	NW	73	305
N78E	29	NW	29	168	N132E	27	NE	27	402

Geomechanics uses the physical and mechanical properties of materials. Thus, the density or specific weight of the rock on the one hand, and the stresses at breakage, cohesion and the angle of internal friction on the other hand. The focus of our study is solely on the stability of the northwestern flank of the Ruashi II mine. For this purpose, samples were taken from different formations on the mine flank to be tested, namely:

- Laterite;
- Black ore limestone (CMN);
- Altered dolomitic shale (Saprolite)

Rock mass classification systems represent an important tool often used for the preliminary evaluation of the technical behavior of the rock mass [**16**]. In the framework of this study, we will focus on the Rock Mass Rating (RMR) of Bieniawski 1989 to classify the rock mass [**17**] [**18**].

The description of hole RGT1 of Ruashi upstream of the landslide zone of coordinates 559485.561; 8714911.692; 1281.934 is used to determine the CMA according to five parameters and to classify the Ruashi rockmass (**see Table 3**).

Table 3: Summary of the result of the survey description

Training	Is	RQD	Js	Jc	Jw	CMA
Saprolite	1	5	5	1	7	19
CMN	7	13	9	10	15	54

The results show that Saprolite belongs to class V materials with a value lower than 20 (very bad) while CMN belongs to class III materials with a value between 60 and 41 (good) [**17**]. Since Saprolite is predominant in the flank formation, these materials are assimilable to the soil. Hence the choice of Bishop as the analytical model for the simulation [**19**]. With (RMR: Rock Mass Rating), (Is: FranklinIndex), (RQD: Rock Quality Designation), (Js: JointSpacing), (Jc: Joint Nature), (Jw:Water Flow).

The laboratory tests determined the effective parameters for a long-term stability study. The tests are made for the deduction of normal stress (σ) and shear stress (τ), cohesions (C) and internal friction angles (ϕ). The average density weights (γ) are taken from the studies of the implementation of geotechnical data of the city of Lubumbashi [**20**]. The above mentioned parameters in **table 4**.

Table 4: Mechanical parameters and intrinsic characteristics of the soil

Formation	Σ[kPa]	τ [kPa]			
Latérite	34,70	67,23	φ[°]	C[kPa]	γ[kN/m^3]
	52,07	78,46	32,10	45,57	15,64
	69,40	89,00			
Saprolite	34,70	113,23	φ[°]	C[kPa]	γ[kN/m^3]
	52,07	116,77	10,674	106,78	19,28
	69,40	119,77			

The knowledge of the effective normal stress and the shear strength of two specimens allows the determination of the points of the intrinsic curve, whose ordinate at the origin represents the effective cohesion of the material and its slope the angle of internal friction as shown in **Figure I**.

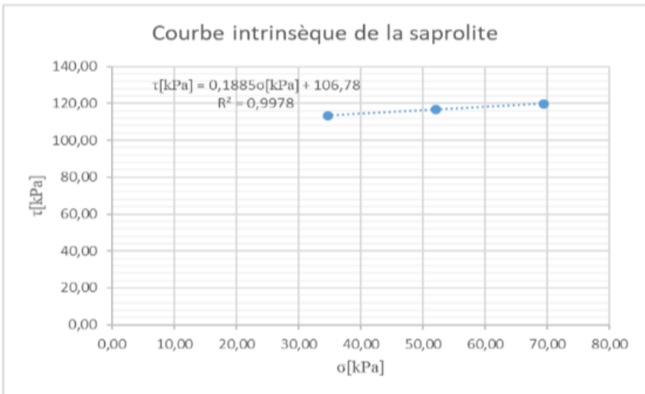

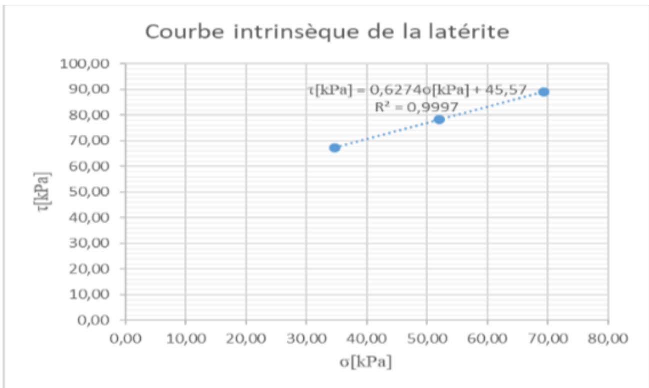

Figure I: Intrinsic soil curves (Saprolite and Laterite)

The cohesion and the internal angle of friction are determined by the values of the compressive and tensile strength [**21**]. The results presented in table 6 are based on the rock of black ore limestone, especially the cohesion, the internal angle of friction and its specific weight.

Table 6: Intrinsic Characteristics of Black Ore Limestone.

Parameter	Average Value
Cohesion	286.75 kPa
Internal angle of friction	30°
Specific weight	31.95 kN/m^3

Several classifications of slope movement exist and they are based on the nature of the terrain, water content, kinematics of the movement etc. The shape of the sliding surfaces depends much more on the characteristics of the material. Based on the kinematics of motion and the morphology of failure surface, [**22**] [**18**] counts the cases of slope sliding (plane failure; wedge failure; tilting failure; and rotational or circular failure). Its analysis is commonly used to predict potential mechanisms of structural instability using stereonets methods. In this paper, we treat the case of circular failure because the rock is highly altered and the rockfall occurred in the upper part of the mine which is essentially composed of altered rocks with soil behaviour [**19**].

3. Results and Discussion

1) *Geostructural modeling*

Numerical modeling is used for slope geometries, more complex failure mechanisms and provides insight into the effect of stress distribution in the slope and displacements on its behavior. As a mode of representation of discontinuities, we use spherical projection [**23**]: Lambert projection using Schmidt's framework and stereographic projection using Wulff's framework.

The geometrical constructions are practically the results of the digitization in Dips which shows the observation of the concentration of poles around the points as well as the preferential families of discontinuities are presented in **Figures II to VIII**.

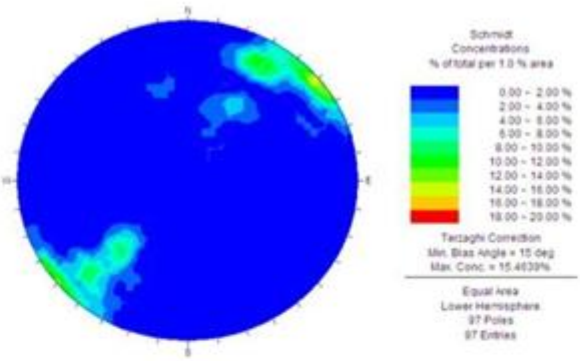

Figure II: stereogram of densities of 96 poles of stratification

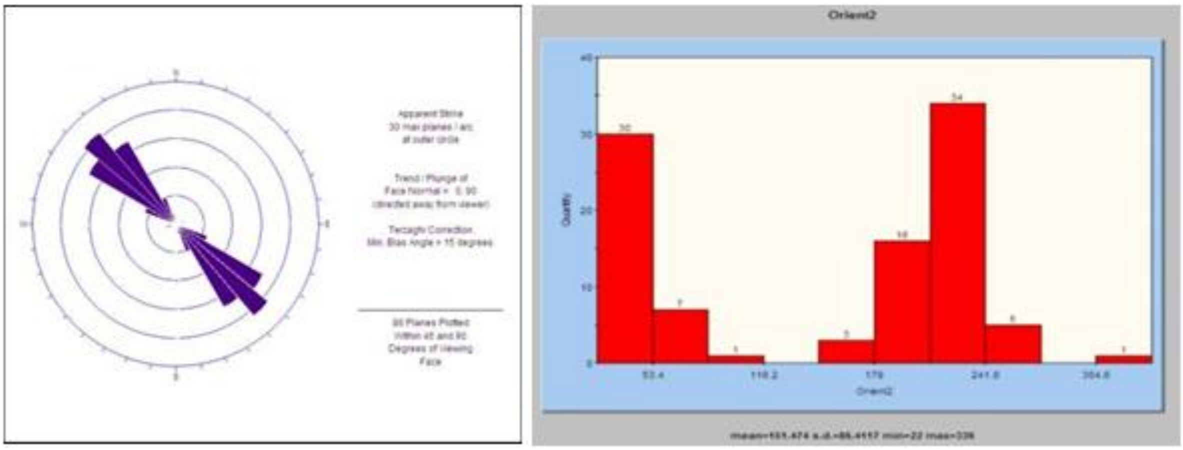

Figure III: Rosace of stratification measurements (left) and histogram of stratification measurements (right)

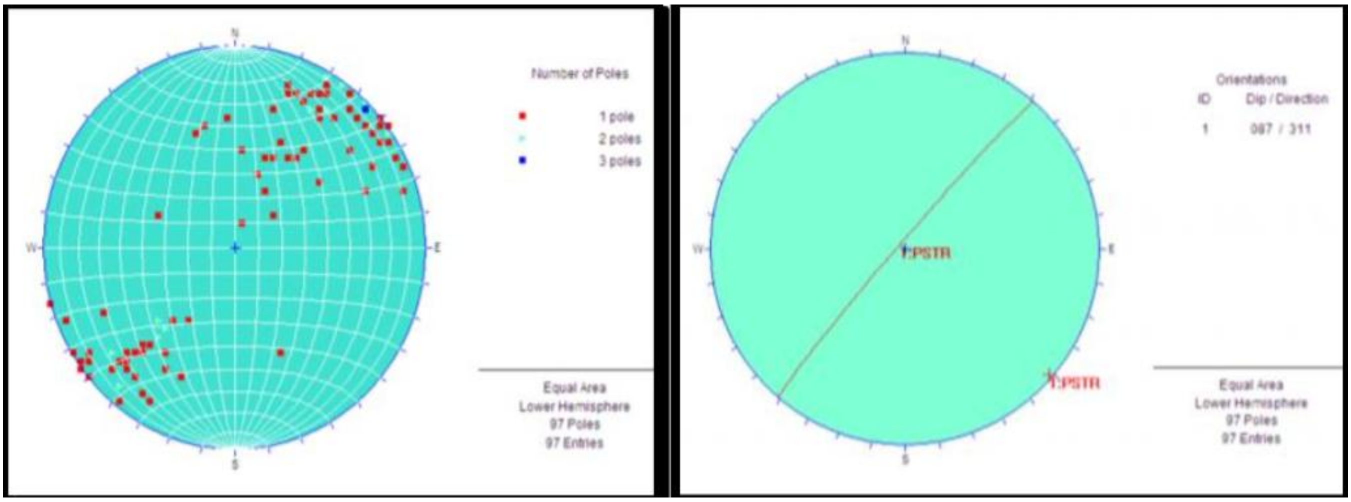

Figure IV: Pole distribution of the stratification surfaces (left) and representative stratification plane (right)

ISSN: 2319-7064
ResearchGate Impact Factor (2018): 0.28 | SJIF (2019): 7.583

At the end of the treatment of ninety-seven measures (97) of the stratification designs, we found a single family of stratification designs whose orientation parameters show 87/311 according to the English notation. The histogram of the stratification measurements shows that the considerable quantity of these measurements has directions between 210° and 245°, i.e. 35% **Figure III** on the right.

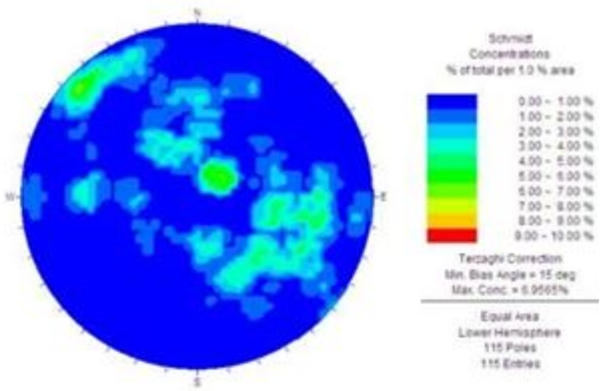

Figure V: Stereogram of 115 pole break densities

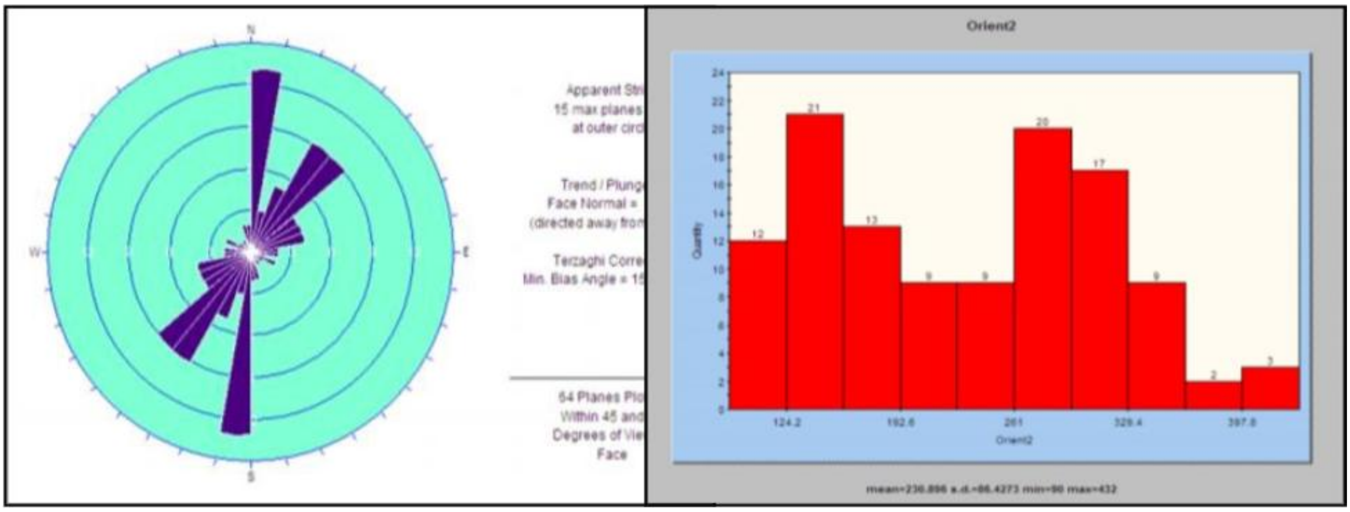

Figure VI: Rosace of break plane measurements (left) and histogram of break measurements (right**)**

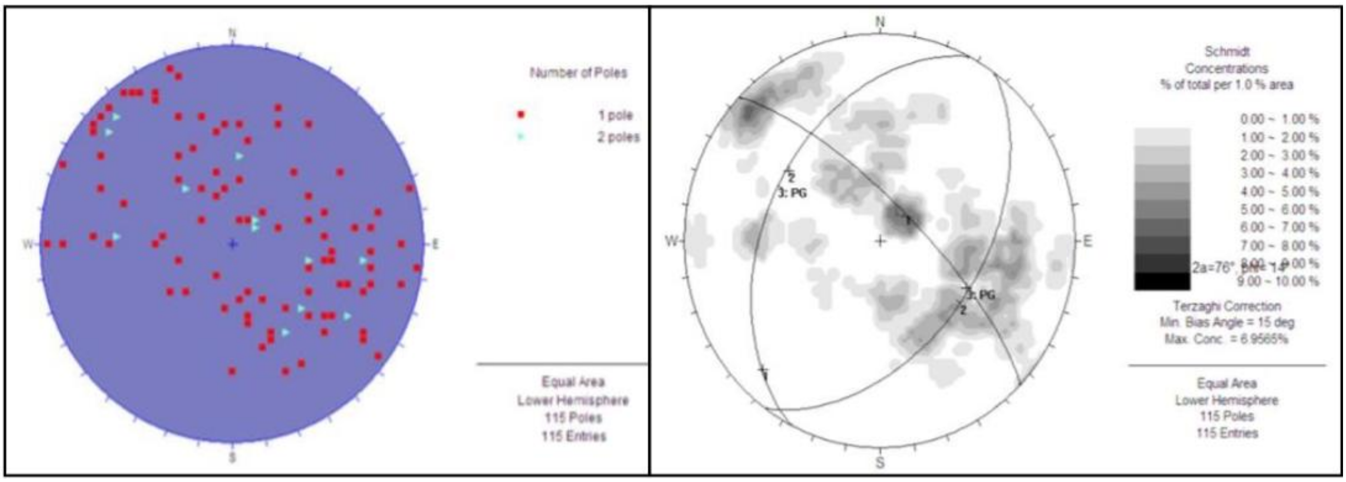

Figure VII: Breakage pole distribution (left) and representative break planes (right).

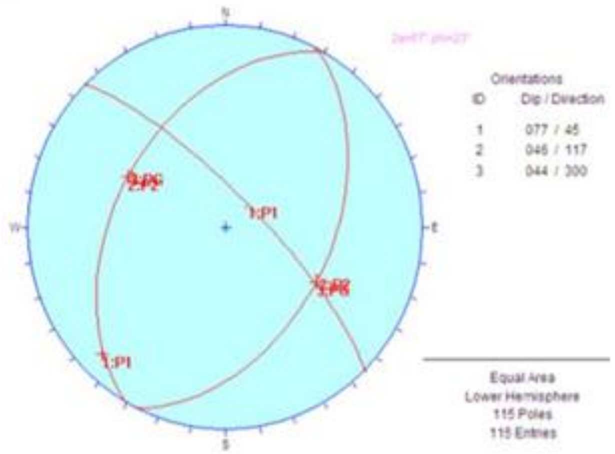

Figure VIII: Representative drawings of the *breaks* and estimation of the *internal angle of friction*.

The treatment of one hundred and fifteen measures of breakage discriminates between two types of families whose orientation parameters are 77/45 and 46/117 respectively for the first plane and the second plane and a sliding plane whose orientation parameters are 44/300. The histogram of break measurements shows that break measurements in directions between 124° and 159°, i.e. 18%, are in large quantity (Figure Von the right). And we have estimated an internal angle of friction phi which amounts to twenty-three degrees (ϕ=23° see figure VIII). After analysis, we found that the slip is oriented towards the west.

2) *Geomechanical modeling*

The limit equilibrium method compares the amplitudes of the driving and resistance forces acting along the sliding planes to estimate the factor of safety Coggan et al. 1998 in [**18**], and it is also widely used to examine the structural stability of slopes. The Slide software is exploited for the simulation of this analysis, from the sections of the two-dimensional geometric model created on the digital terrain model (DTM) of the Ruashi mine.

Two cuts were made, one on the extreme West with the following coordinates derived from the top and bottom points of the discovery where the cut plane passes through (Y=8714789.503; X=559375.010; Z=1292.668), (Y=8714780.344; X= 559688.588; Z=1292.668) and the other at the extreme North with the coordinates of the top and bottom points of the cut plane respectively:(Y= 8715232.096; X= 559696.392; Z= 1271.092) and (Y= 8715115.267; X= 559714.887; Z= 1218.518). It should be noted that the analysis is done by the simplified Bishop method over a slump height of approximately 77 metres. The results of the analysisby two approaches (deterministic and probabilistic) on heterogeneous geological formations a Saprolite surmounted by a layer of laterite are presented on **figure X**.

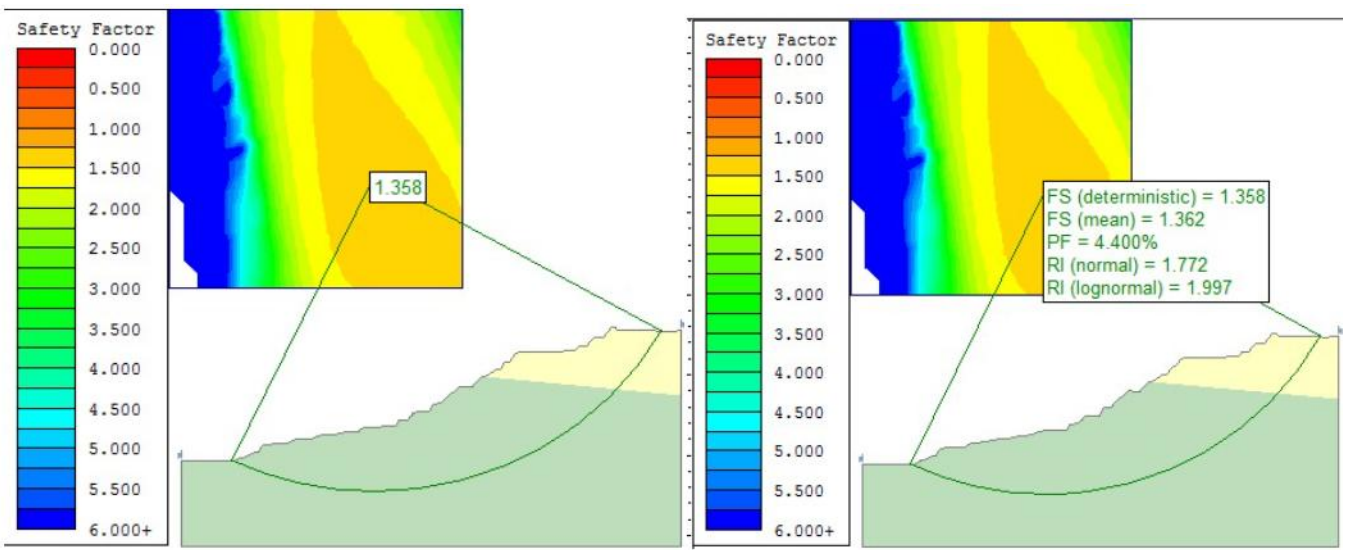

Figure IX: Presentation of the Western Logging Security Factor.

The sensitivity of the materials shows that an increase in the specific weight of Saprolite slightly decreases the safety factor, on the other hand the lines of cohesion and the internal angle of friction are almost stiff whatever the increase of the latter. **Figure X** shows the sensitivity of this analysis.

International Journal of Science and Research (IJSR)
ISSN: 2319-7064
ResearchGate Impact Factor (2018): 0.28 | SJIF (2019): 7.583

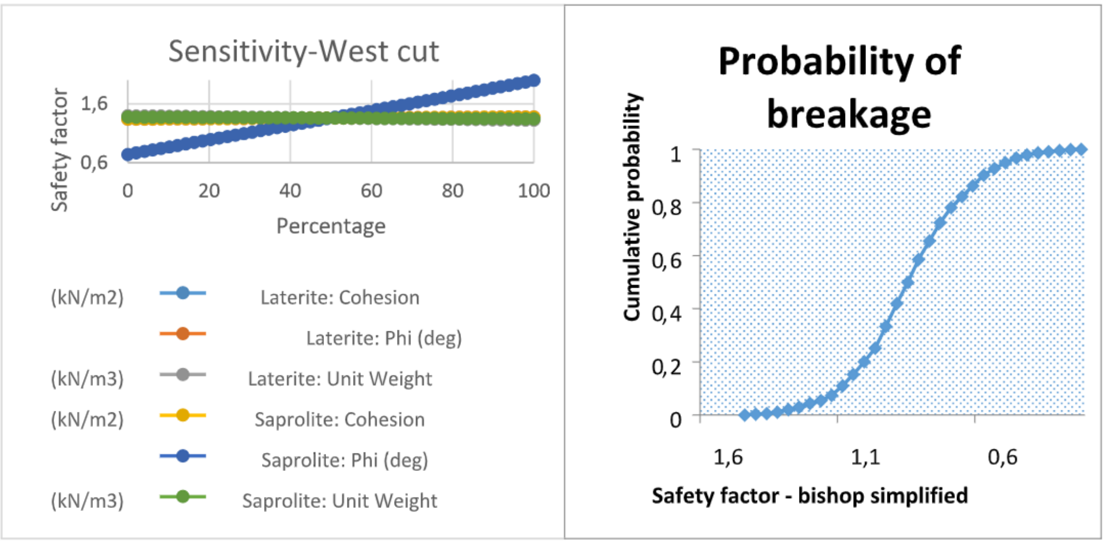

Figure X: Sensitivity of the geomechanical parameters and the evolution of the probability of the western cut.

The distribution function of the geomechanical parameters of the Saprolite surmounted by the Laterite shows for this cut, a probability of 51.38% of stability for the slices with a safety factor of 1.362.

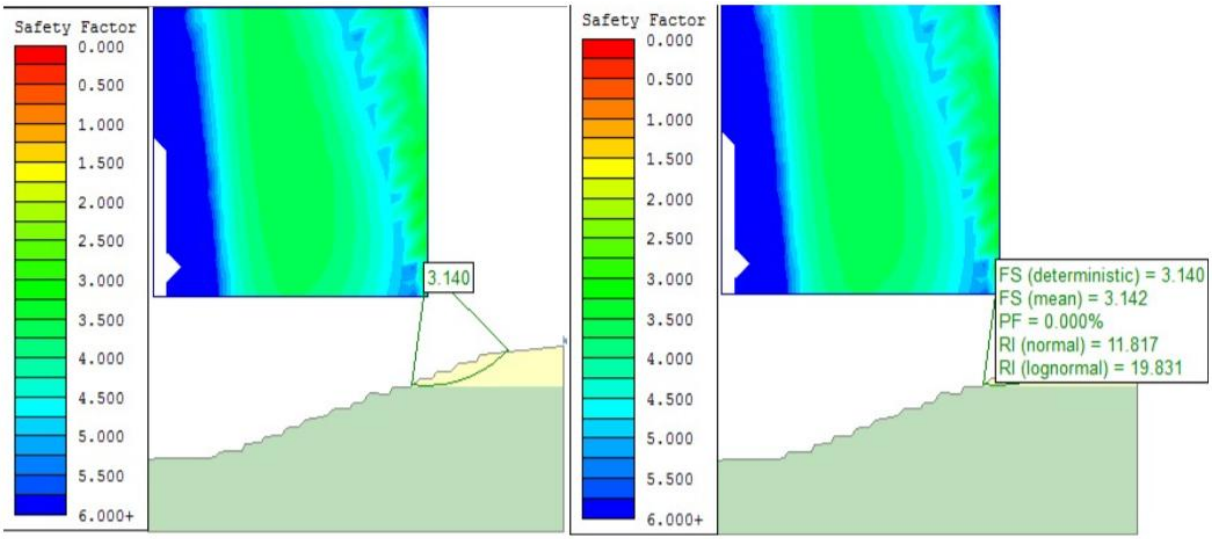

Figure XI: Presentation of the Safety Factor for the North cut

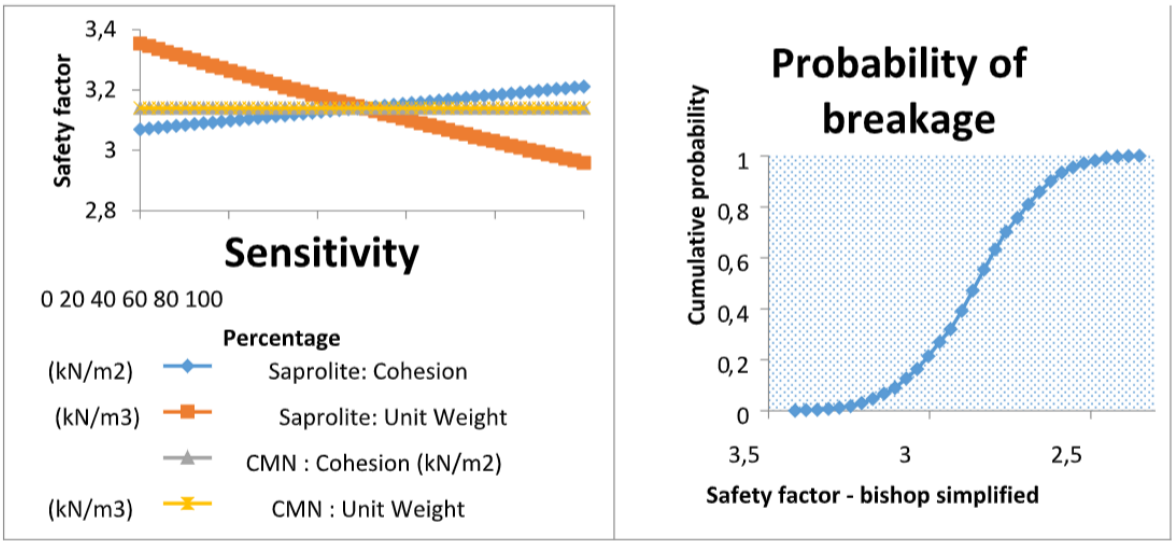

Figure XII: Sensitivity of the geomechanical parameters and the evolution of the probability of the North cut.

The sensitivity of the parameters of the north cut, makes us observe that the more the cohesion increases, the more the safety factor increases, on the other hand, the more the specific weight increases, the more the safety factor decreases and the other straight lines are steep.

The distribution function shows that units with a safety factor of 3.142 have a 48.85% probability of breakage.

4. Conclusion

Structural measures of fractures and breaks discriminated three families. A westward sliding plane was established from two fracture planes with 44/300 as orientation parameters. This also made it possible to estimate a structural angle of friction of 23°. Samples collected on the flank show that the rock is mostly altered shale (Saprolite) to the west, but towards the north, the black ore limestone rock is average quality. The digitization of the site by performing two cuts shows agood safety factor which means that the flank is stable. Upon inspection of the mine upstream of the northwestern flank of Ruashi II zone adjacent to Ruashi I, there are a significant number of cracks. Thus [**23**] shows that water reduces the shear strength along the potentially fractured slope surfaces (joints, faults etc.). Meteoric runoff water in the tensile cracks between the two mines would have caused saturation of the materials by decreasing cohesion and an increase in specific weight with a significant decrease in the safety factor. In view of the influx of runoff water that threatens the Ruashi mine in general and Ruashi II in particular, [**19**] [**6**] proposes the following measures to improve the safety factor. In the context of this pit, we opt for surface drainage of runoff and percolation water to reduce the water content in the traction cracks. This is complemented by the excavation of gullies upstream of the unstable zone and drainage at the foot of the bleachers. A study is underway that will take into account dynamic, static and hydrostatic stresses and traction cracks or their couplings.

References

[1] Kamulete M., (2009), Cours *d'Exploitation des mines à ciel ouvert*, Presses Universitaires de Lubumbashi (PUL), Lubumbashi, p4;

[2] Safety work Australia, *Draft ground control in open pit mines*; July 2011; MEUR P.-Y., COCHONAT P., DAVID C., GERONIMI V., SAMADI S. (coord.), 2016 *Les ressources minérales profondes en Polynésie française. Marseille*, IRD Éditions, coll. Expertise collégiale ISBN: 978-2-7099-2191-6.

[3] Descamps et al, (2014), *Contribution au développement de l'exploitation rationnelle des gisements miniers congolais*, KAOW- ARSOM, Royal *Academy* of Overseas Sciences, First Young *Researchers Oversea's* Day, Brussels-Belgium;

[4] Call R.D et JP Savely (1990), *Open* Pit *Rock mecanique. Surface* mining,2e edition. Society of mining, metallurgy and exploration,Inc. Pp 860-882.B.A. Kennedy ed.

[5] Girard,J.M. , P.E., C.M.S.P, *Assessing and monitoring open pit mine highwalls* , National Institute for Occupational Safety & Health, Spokane Research Laboratory, 315 E. Montgomery Ave., Spokane, WA 99207. http://www.cdc.gov/niosh 2020.08.22;

[6] Charline Julio. *Conditioning of* the *stochastic 3D modeling of fault networks*. Earth Sciences. University of Lorraine, 2015. NNT: 2015LORR0254. Tel-01754539.p1;

[7] Gabriel Godefroy (2018). *Kinematic and stochastic modeling of faults from scattered data for the analysis of structural uncertainties*. Earth Sciences. University of Lorraine, France. NNT: 2018LORR0052. tel-01809508.pp 224 -29;

[8] Mohammed Ali et al. *Rock slope assessment using kinematic and numerical analyses.* Jurnal Teknologi (Sciences & Engineering) 72 :1 (2015) 1-6

[9] Gautier Laurent (2013) *Taking into account the tectonic history of geological structures in the creation of compatible 3D digital models*. PhD thesis University of Lorraine. p 13;

[10] SOILS - MEASUREMENT (2015), *Soil Mechanics*. Geotechnics and Agronomy http://www.sols-mesures.com 2020.09.03

[11] AFNOR (2000), *Détermination de la résistance à la compression uniaxiale*, Tour Europe 92049, Paris La Défense Cedex, ISSN 0335-3931;

[12] Pierre POTHÉRAT, (1998), *Use of* the Tectronic *4000 electronic compass for geological and structural studies.* Bulletin des Laboratoires des Ponts et Chaussées - 214 - March-April 1998 - REF NT 4190 - PP 97-101;

[13] Rocscience Inc. Dip v. 6.0 - *Graphical and statistical analysis of orientation data*. Toronto, Canada. 2014;

[14] Erik Eberhardt, *Rock slope stability Analysis-Utilization of advanced- numerical Technique*. Geological Engeneering/EOS UBC- Vancouver, Canada. April, 2003

[15] Duran A, Douglas K. *Experience with empirical rock slope design*. In: proceedings of ISRM International Symposium; 2000.

[16] J. A. Hudson and J. P. Harrison (1997), *Engineering rock mechanics: an introduction to the principles*, Pergamon, Elsevier Science Ltd, Oxford OX5 IGB, UK;

[17] H. Basahel and H. Mitri. *Application of rock mass classification systems to rock slope stability assessment: A case study*, Journal of Rock *Mechanics* and *Geotechnical* Engineering; 9 (2017) 9931009.

[18] Mohamed KHEMISSA, *Methods of stability analysis and slope stabilization techniques*. Journées Nationales de Géologie et de Géotechnique de l'Ingénieur JNGG Lyon, France 27-29 June 2006.p15;

[19] Kasongo et al (2018), *Elaboration de la carte géotechnique de la ville de Lubumbashi guide technique de sélection des sites d'implantation d'ouvrages du génie civil*, Europan Scientific Journal, Edition vol.14, N°36 ISSN: 1857-7881(Print) e-ISSN1857-7431;

[20] D. Cordary (1994), *Mécanique des Sols*, Lavoisier- Tec and Doc, Paris;

[21] E.Hoek (1995), *Practical Rock Engineering*, A.A. Balkema Publishers, Old Post Road, Brookfield, VT 05036-970, Canada;

[22] Duncan C. Wyllie and Christopher W. Mah, (2004) *Rock Slope Engineering Civil and mining*, 4th edition, Spon Press Taylor & Francis Group, London and New York, pp28-30.